Journal of Academia Vol. 14, Issue 1 (2026) 10 – 22

Dissolution of Zinc Oxide Using Choline Chloride-Based Deep Eutectic Solvents with Various Hydrogen Bond Donors

Samer Sami Aburub[1,2], Nur Aida Mohd Zakhir[1], Nurul Yani Rahim[1*]

[1]*School of Chemical Sciences,*
Universiti Sains Malaysia (USM), Kampus Induk, 11800 USM, Pulau Pinang, Malaysia
[2]*Department of Pharmaceutical Chemistry, College of Pharmacy,*
Najran University, 11001 Najran, Saudi Arabia

[*]*Corresponding author: nurulyanirahim@usm.my*

Abstract

Metal oxides (MO) are essential in various industrial applications, yet their limited solubility in common solvents often hinders their utility. This study investigates the dissolution of Zinc Oxide (ZnO) using green and cost-effective deep eutectic solvents (DESs) composed of Choline Chloride (ChCl) as a hydrogen bond acceptor (HBA) paired with three different hydrogen bond donors (HBDs): Ascorbic Acid (AA), Maleic Acid (MA), and Urea. The synthesized DESs were characterized using Fourier-transform infrared (FTIR) spectroscopy, thermal gravimetric analysis (TGA), and differential scanning calorimetry (DSC) to confirm hydrogen bond formation and thermal stability. Dissolution experiments were conducted to evaluate the effects of HBD type, ZnO mass, heating time, and temperature, with zinc concentrations measured via atomic absorption spectroscopy (AAS). The results indicate that ChCl:AA (2:1) exhibits the highest dissolution ability, achieving a dissolution efficiency of 80.6% at 5 mg of ZnO, significantly outperforming ChCl:MA (2:1) at 71.4% and ChCl:Urea (1:2) at 77.4% under identical conditions. While both ChCl:AA (2:1) and ChCl:MA (2:1) were capable of dissolving a maximum mass of 20 mg of ZnO, the superior efficiency of ChCl:AA is attributed to its unique chemical properties as a reducing agent and its capacity to form stable, soluble zinc ascorbate complexes. The optimum dissolution parameters were identified as 70 °C for 48 hours for ChCl:AA (2:1), 60 °C for 18 hours for ChCl:MA (2:1), and 80 °C for 48 hours for ChCl:Urea (1:2). These findings highlight the potential of acid-based DESs, particularly those with complexing capabilities like ChCl:AA, as effective and sustainable solvents for metal oxide dissolution.

Keywords: dissolution; metal oxides; deep eutectic solvents

Article History:- Received: 17 July 2025; Revised: 7 January 2026; Accepted: 11 February 2026; Published: 30 April 2026

DOI: https://doi.org/10.24191/joa.v14i1.7591

Introduction

Metal oxides (MO) are widely employed in many industries, including catalysis, energy storage, and biomedical engineering. They are also widely distributed in nature and can be found in soils, rocks, and minerals. For instance, many rocks and soils contain iron oxide (Fe_2O_3), which is the primary ingredient in rust (Taghizadeh et al., 2020). MOs like zinc oxide (ZnO) and titanium dioxide (TiO_2) are utilized as photocatalysts in applications including solar energy conversion and water purification. In numerous industries, including electronics, optoelectronics, and catalysis, ZnO is a particularly important MO due to its exceptional properties, such as high electron mobility, high thermal conductivity, and a wide direct band gap (Noman et al., 2022). However, a significant challenge remains in its limited solubility in common solvents, which can restrict its processing and application.

The conventional method for dissolving MOs often involves strong acids like sulfuric or hydrochloric acid. This approach has major drawbacks, including the production of toxic waste products that can lead to soil acidification and water pollution if not managed properly (Li et al., 2021). Furthermore,

some MOs, such as silicon dioxide (SiO_2) and aluminum oxide (Al_2O_3), are extremely difficult to dissolve even in potent acids, requiring harsh conditions like high temperatures and pressures. To overcome these limitations, alternative solvents have been explored. Ionic Liquids (ILs), which consist of an organic cation and an organic or inorganic anion, have shown great promise due to their high thermal stability, low volatility, and excellent solubility for some MOs (Sakhno et al., 2020). However, their widespread industrial use is often constrained by their high manufacturing cost and potential

toxicity (Markiewicz & Jurga, 2011). As a more sustainable alternative, DESs have recently attracted significant attention. Formed by mixing a hydrogen bond donor (HBD) and a hydrogen bond acceptor (HBA) to create a eutectic mixture with a low melting point, DESs offer several advantages over ILs, including lower cost, reduced toxicity, and greater biodegradability, as they are often synthesized from renewable sources (Ling & Hadinoto, 2022). Despite their potential, the dissolution behavior of MOs in DESs is not yet well understood, and more research is required to optimize the process and explore the full range of their capabilities (Richter & Ruck, 2020).

In this study, DESs made of choline chloride (ChCl) and several HBDs including ascorbic acid (AA), maleic acid (MA), and urea were synthesized and used to examine the dissolution of ZnO. These specific HBDs were selected because, to the best of our knowledge, their ability to dissolve ZnO in a DES formulation has not been previously reported. The solubility of ZnO was investigated as a function of HBD type, mass of ZnO, time, and temperature. The findings of this work aim to provide critical insights into the dissolution behavior of ZnO in these novel DESs and to establish optimal conditions, thereby advancing their potential application as environmentally friendly solvents in various industrial fields.

Methods

Materials

Choline chloride, $C_5H_{14}NO{\cdot}Cl$ (≥ 98%) was purchased from Sigma-Aldrich (China). Ascorbic acid, $C_6H_8O_6$ was purchased from J. T. Baker (Japan). Maleic acid, $C_4H_4O_4$ was purchased from Merck (Germany). Urea, CH_4N_2O was purchased from R&M Chemicals (United Kingdom). Zinc oxide, ZnO was purchased from Univar (United States). Hydrochloric acid, HCl (37%, Grade AR) was purchased from QReC (Malaysia). Zinc standard for AAS (1000 mg/L ± 4 mg/L) was purchased from Sigma-Aldrich (Switzerland). All experiments were carried out using distilled water.

Instruments

The raw materials and DESs were scanned by using Fourier-transform infrared (FTIR, Frontier, PerkinElmer, USA) spectroscopy at a resolution of 4 cm^{-1} in the wavenumber range of 4000 cm^{-1} to 600 cm^{-1}. Thermogravimetric analysis (TGA) was performed to evaluate the thermal stability of the prepared DESs and their pure constituents using a STA 6000 instrument (PerkinElmer, USA) in the temperature range of 30–500 °C at a heating rate of 20 °C/min. Differential scanning calorimetry (DSC) measurements were carried out using a DSC 3500 Sirius instrument (NETZSCH, Germany) over a temperature range of –30 to 250 °C at a heating rate of 20 °C/min to investigate the thermal behavior of the DESs.The pH of the DESs were determined by the pH meter (HI-5221, HANNA, USA). The concentration of Zn dissolved in DESs were determined using atomic absorption spectroscopy (AAS, analyst 400, PerkinElmer, USA) at wavelength 213.86 nm where 0.2, 0.4, 0.6, 0.8 and 1.0 ppm of Zn standard solutions were prepared for calibration curve.

Synthesis of DESs

Choline chloride (ChCl) was selected as the HBA due to its low cost, biodegradability, low toxicity, and widespread use in DES systems. Ascorbic acid (AA), maleic acid (MA), and urea were chosen as HBDs based on their strong hydrogen-bonding ability and chemical diversity, allowing evaluation of different functional groups on DES formation and properties (Chik et al. 2025). The selected HBA:HBD molar ratios for DES preparation are summarized in Table 1**.** The molar ratios of ChCl:AA (2:1) and ChCl:Urea (1:2) were chosen based on reported literature and preliminary experiments, which confirmed the formation of stable and homogeneous liquid phases. In contrast, the ChCl:MA system

was found to be highly sensitive to the HBA:HBD ratio; therefore, multiple molar ratios (1:1, 2:1, and 1:2) were investigated to identify the optimal composition capable of producing a clear and stable DES. The mixtures were heated at 80 °C under continuous stirring until homogeneous clear liquids were obtained, followed by cooling to room temperature and storage for further characterization. Figure 1 shows the synthesized DESs. For ChCl:MA, only ratio 2:1 produce homogeneous clear liquid while the other two ratios produce cloudy mixture.

Table 1. Molar ratio of HBA:HBD for DESs preparation

HBA:HBD	Molar ratio
ChCl:AA	2:1
ChCl:Urea	1:2
ChCl:MA	1:1
ChCl:MA	2:1
ChCl:MA	1:2

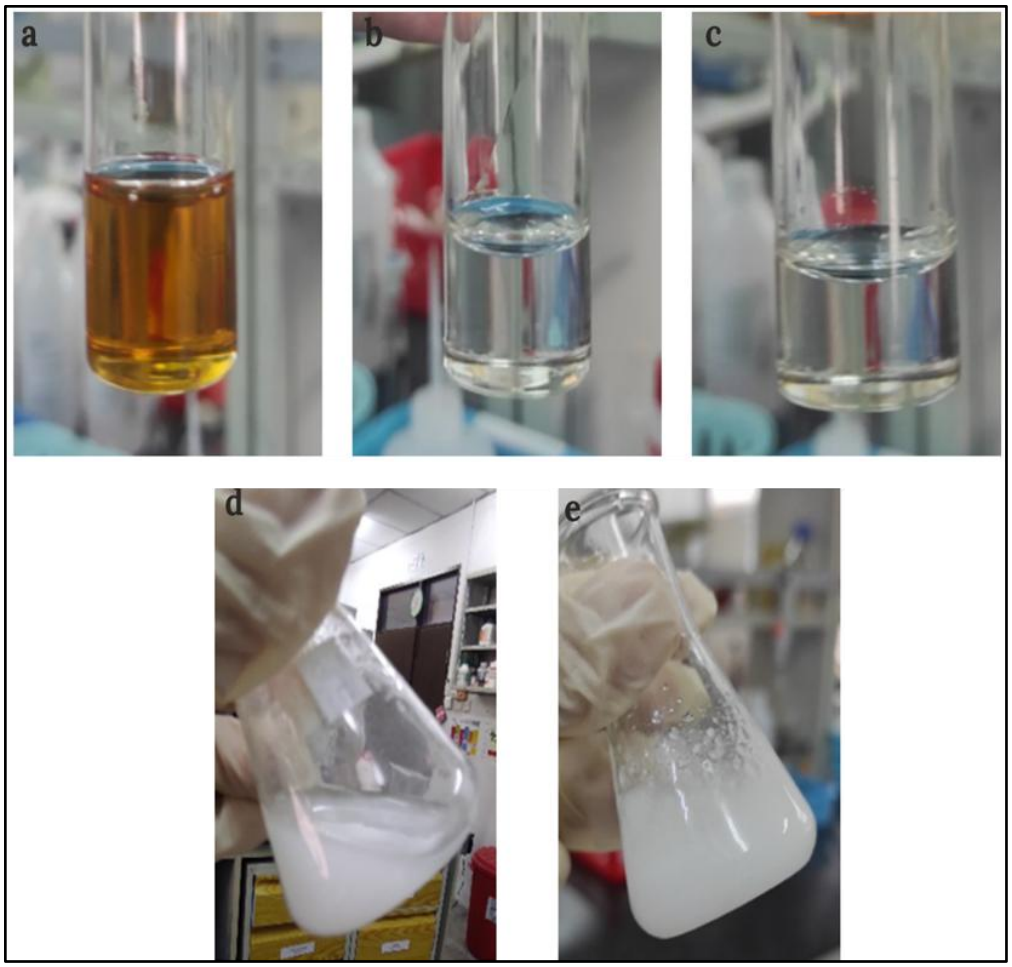

Figure 1. The synthesized DESs of (a) ChCl: AA, (b) ChCl:MA (1:1), (c) ChCl: Urea (d) ChCl:MA (2:1) and (e) ChCl:MA (1:2)

pH determination of DESs

About 2 mL of DES was added into a beaker containing 10 mL of distilled water. The solution was mixed thoroughly until become homogenous. The pH of the DES was determined by dipping the pH electrode into the solution.

Effect of HBD on dissolution of zinc oxide

The method was used from Jangir et al. (2021) with some modification. About 5 mg of ZnO was dissolved in 2 mL of DES. Then, the mixture was heated at 50 °C for 48 hours. ZnO was completely

dissolved after 48 hours. After that, 10 mL of distilled water was added into the mixture to reduce its viscosity and easier to be filtered (Amphlett & Choi, 2019). Then, it was filtered using 0.45 µm nylon syringe filter into 100 mL volumetric flask. The solution was diluted with 2% HCl to the mark.

Effect of mass of zinc oxide to the dissolution

About 5, 10, 15 and 20 mg of ZnO was dissolved in 2 mL of DES in four different flasks. Then, the mixture was heated at 50 °C for 48 hours. Subsequently, 10 mL of distilled water was added into the mixture and then filtered using 0.45 µm nylon syringe filter into 100 mL volumetric flask. The solution was diluted with 2% HCl to the mark.

Effect of heating time on dissolution of zinc oxide

About 5 mg of ZnO was dissolved in 2 mL of DES. Then, the mixture was heated at 50 °C for 18, 20, 24 and 48 hours. After that, 10 mL of distilled water was added into the mixture and then filtered using 0.45 µm nylon syringe filter into 100 mL volumetric flask. The solution was diluted with 2% HCl to the mark.

Effect of heating temperature on dissolution of zinc oxide

About 5 mg of ZnO was dissolved in 2 mL of DES. Afterwards, the mixture was heated at 50, 60, 70 and 80 °C for 18 h (for ChCl:MA) and 48 h (for ChCl:AA and ChCl:urea). After that, 10 mL of distilled water was added into the mixture and then filtered using 0.45 µm nylon syringe filter into 100 mL volumetric flask. The solution was diluted with 2% HCl to the mark.

Analysis of soluble zinc using AAS

The solution was further diluted by taking 500 µL of the solution into 50 mL volumetric flask and 2% HCl was added to the mark. The sample was ready to be run into AAS. Standard of 0.2, 0.4, 0.6, 0.8, and 1.0 ppm were prepared for AAS. The results were presented in the percentage of dissolution by using this formula:

$$\text{Percentage of dissolution} = \frac{\text{dissolved concentration}}{\text{initial concentration}} \times 100$$

Result and Discussion

Fourier-transform infrared (FTIR) spectroscopy analysis

FTIR spectroscopy observed the formation of DESs and interaction between the two molecules of HBA and HBD. The FTIR spectra of ChCl:AA (2:1), ChCl:MA (2:1) and ChCl:Urea (1:2) along with their HBA and HBD are shown in Figure 2 . Figures 2a shows the FTIR spectra of ChCl, AA, and ChCl:AA (2:1). In the ChCl spectrum, distinct spectral features were observed, including a broad band at 3225 cm^{-1} associated with O-H stretching vibration, and a vibration band at 3026 cm^{-1} related to the stretching mode of C-H stretching vibration. A vibration bands at 1479 cm^{-1} which indicated an alkyl group, were also seen, supporting characteristics of ChCl. On the other hand, in the AA spectrum, two distinct spectral features were observed. Firstly, a significant absorption peak at 1754 cm^{-1} was noted, indicating the presence of stretching vibrations of C=O bonds. Second, a strong band at 1652 cm^{-1} was identified, indicating the presence of stretching vibrations associated with C=C bonds.

According to previous literature, hydrogen bonding is essential to produce DESs (Ling et al., 2020). Infrared spectroscopy can show the formation of hydrogen bonds through changes in bond length and the accompanying vibrations of hydrogen bonds. Red-shift when the wavenumbers are shifted to lower wavenumbers generally indicate a weakening or lengthening of the bond, while blue-shifts when the wavenumbers are shifted to higher wavenumbers suggest a strengthening or shortening of the bond (Joseph & Jemmis, 2007). It was clear that the ChCl:AA (2:1) spectrum generally overlapped the ChCl and AA spectra, particularly in the vibration region that corresponds to the amino group (867 cm^{-1} to 1200 cm^{-1}). The O-H stretching vibration bands that were seen at 3225 cm^{-1} in the ChCl spectrum have

shifted to 3270 cm^{-1} in the spectrum of ChCl:AA (2:1). The O-H stretching frequency in DESs is observed to be higher than that of ChCl, indicating a blue-shift in the O-H stretching vibration within DESs (Wang et al., 2019). According to theory, the force constants of the specific bond have a significant impact on the frequency of a normal vibration. A bond length and bond strength can be disturbed by intermolecular interactions such a hydrogen bond leading to changes in the spectral signature. Therefore, the formation of hydrogen bonds between the pure ChCl and AA during the production of the DES is shown by the shifting of the O-H stretching vibration. Furthermore, it is obvious from comparing the spectrum of AA and ChCl:AA (2:1) that the absorption bands of AA in the range of 3200 cm^{-1} to 3600 cm^{-1} develop bigger and broader bands in ChCl:AA (2:1) spectrum. This observation can be explained by the formation of hydrogen bonds between AA and ChCl, which leads to a distribution of different bond lengths and strengths. Because of this, the O-H group experiences a wide range of vibrational frequencies as opposed to only one obvious frequency. This dispersion causes the O-H stretching vibration band to widen. Additionally, the hydrogen bonding network in DESs can lead to modifications in the environment around the O-H groups, influencing the strength of the hydrogen bonds as well as the overall structure of the solvent. The O-H vibration band is being widened more because of these structural alterations.

As shown in Figure 2b, the FTIR spectra of MA and ChCl:MA (2:1) display multiple peaks between 1650 cm^{-1} and 1700 cm^{-1}, corresponding to the two C=O groups present in maleic acid. The vibrational frequencies observed between 800 cm^{-1} and 1428 cm^{-1} in the structures of the acids, which correspond to the hydroxyl and alkane groups, signify the stretching of C-O bonds, bending of O-H bonds, and stretching of C-H bonds. A comparison of the spectral characteristics of the synthesised DESs and its component parts is necessary to pinpoint the structural modifications and new interactions amongst the compounds. The shift in the carboxylic group peaks at 1703 cm^{-1} in MA to 1715 cm^{-1} in ChCl:MA (2:1) can be seen by comparing the spectra. Furthermore, the occurrence of wider peaks of N-H stretching in the ChCl:MA (2:1) spectra between 2500 cm^{-1} and 3500 cm^{-1} suggests the formation of a hydrogen bond between the nitrogen in the amine group from ChCl and the hydrogen from the carboxyl group in the MA (Al-Risheq et al., 2021). The results reported in this study demonstrate that new hydrogen bonds were formed in the DESs that was synthesised.

As shown in Figure 2c, the FTIR spectrum of pure urea, which possesses an amide structure, exhibits characteristic N–H stretching bands at 3427 cm^{-1} and 3329 cm^{-1}, while the prominent peak at 1589 cm^{-1} corresponds to N–H bending vibrations. C-N stretching, and carbonyl C atom (C=O) were detected at 1456 cm^{-1} and 1663 cm^{-1} respectively. By comparing the IR spectra of pure urea and ChCl:urea (1:2), the stretching of N-H in urea corresponds to the vibrational bands at 3427 cm^{-1} and 3329 cm^{-1} had shifted to 3317 cm^{-1} and 3187 cm^{-1}, respectively, showing hydrogen bonding between urea and choline (Li et al., 2022). Moreover, the bending of N-H at 1663 cm^{-1} and 1589 cm^{-1} in the FTIR spectra of urea also had shifted to 1664 cm^{-1} and 1605 cm^{-1}, respectively in the FTIR spectra of ChCl:urea (1:2) can be attributed to the formation of intermolecular hydrogen bonds between urea and ChCl. The most significant changes in the ChCl:urea (1:2) spectrum were found in these IR regions that are crucial for hydrogen bond formation. Regarding ChCl:urea (1:2), there are only two bands in the carbonyl vibration range, specifically at 1605 cm^{-1} and 1664 cm^{-1}.Additionally, there is a single band at 3187 cm^{-1} indicating the stretching N-H vibration, accompanied by a distinct shoulder at a lower frequency. The observed shifts point to the potential for hydrogen-bound compounds to develop in this DES. ChCl was linked to the CH_3 corresponding band at 1440 cm^{-1} of the ChCl:urea (1:2). The Ch^+ structure was preserved in ChCl:urea (1:2) without being destroyed, as evidenced by the stretching of C-C=O at 953 cm^{-1} in the spectrum. Furthermore, the band at 788 cm^{-1} was attributed to C-H bending in the ChCl:urea (1:2). In eutectic combinations of urea and ChCl, urea can function as both a donor and acceptor in the hydrogen bonding. Previous studies predicted that urea may interact with both choline and chloride ions through several reasonably strong double ionic hydrogen bond interactions (Jurić et al., 2021). Jurić et al. (2021) also stated that the observation of fewer bands in this system lends support to the idea that the stabilisation of eutectic mixtures and charge redistribution within the system are influenced by a dynamic set of hydrogen-bonded interactions. Additionally, both the HBD and HBA have maintained the structure they have because some of the peaks can be seen in both constituent parts and the DESs

spectra. For instance, all DESs' spectra show the peak observed at 627 cm^{-1} indicates the presence of the halogen component in ChCl.

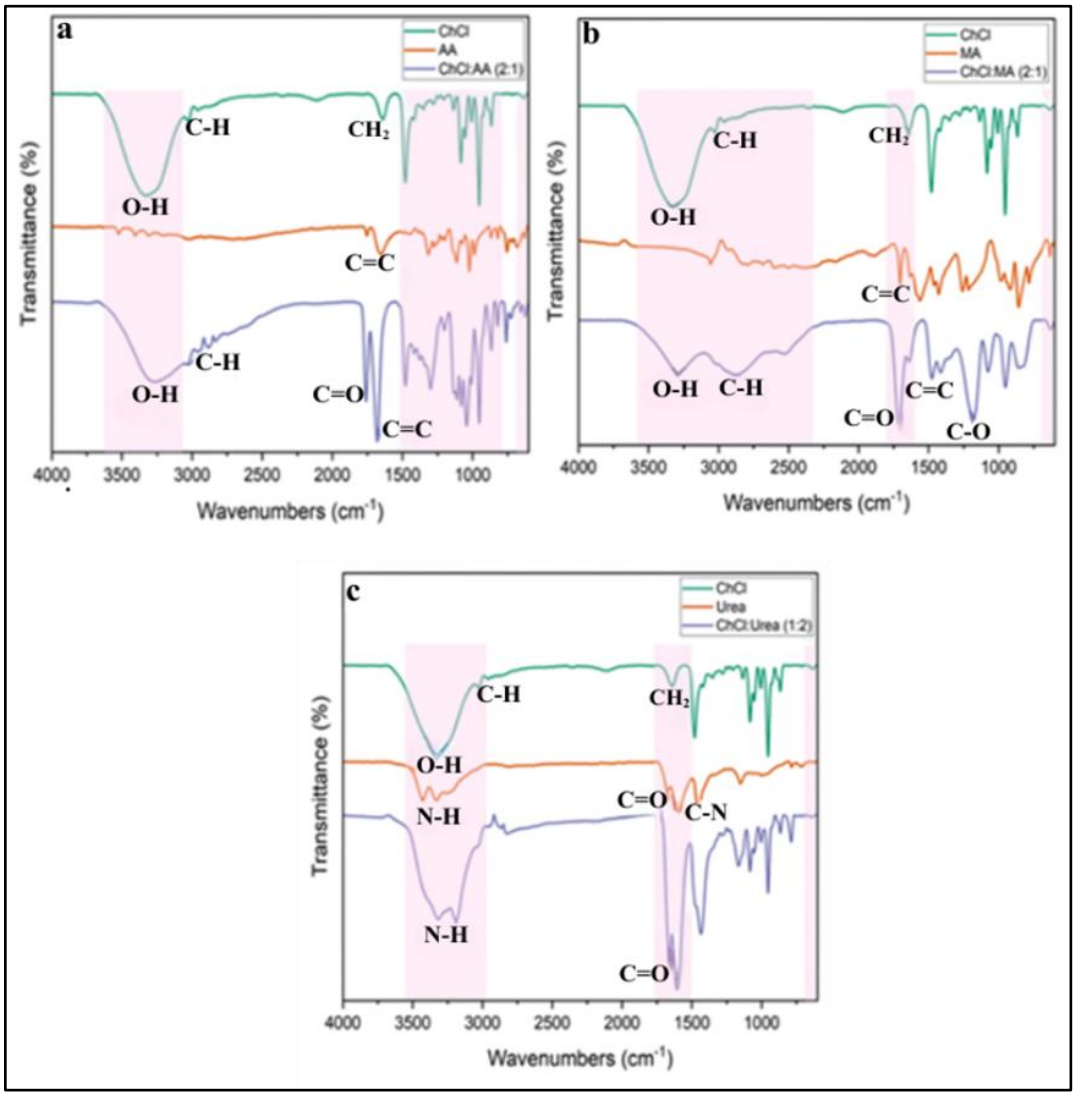

Figure 2. The FTIR spectra of ChCl, AA, and ChCl:AA (a), ChCl, MA and ChCl:MA (b), and ChCl, Urea and ChCl:Urea (c)

Thermogravimetric Analysis (TGA)

The TGA curves of the DESs and their pure constituents are shown in Figures 3. ChCl exhibited a weight loss step at 311.67 °C. As shown in Figure 3a, AA displayed a single weight loss step at 203.85 °C, while the decomposition of ChCl:AA started at 215.95 °C. In Figure 3b, MA also showed one weight loss step at 148.92 °C, whereas ChCl:MA began to decompose at 236.42 °C. In Figure 3c, urea shows weight loss at two steps. At a temperature of 198.75 °C, the initial decomposition of urea takes place, resulting in the formation of ammelide, biuret, and cyanic acid (Delgado-Mellado et al., 2018). This step causes a mass loss of 32.5%. Subsequently, according to Delgado-Mellado et al. (2018), at 325.82 °C, the second decomposition of urea initiates, leading to the complete decomposition of the cyanuric acid derived from biuret. The TGA curve of ChCl:urea exhibited a weight loss at 257.74 °C. The TGA results indicated that the DESs exhibited greater thermal stability than their pure HBD since the higher decomposition temperature observed in the DESs compared to their pure HBD. These results confirmed the interaction between HBDs and ChCl.

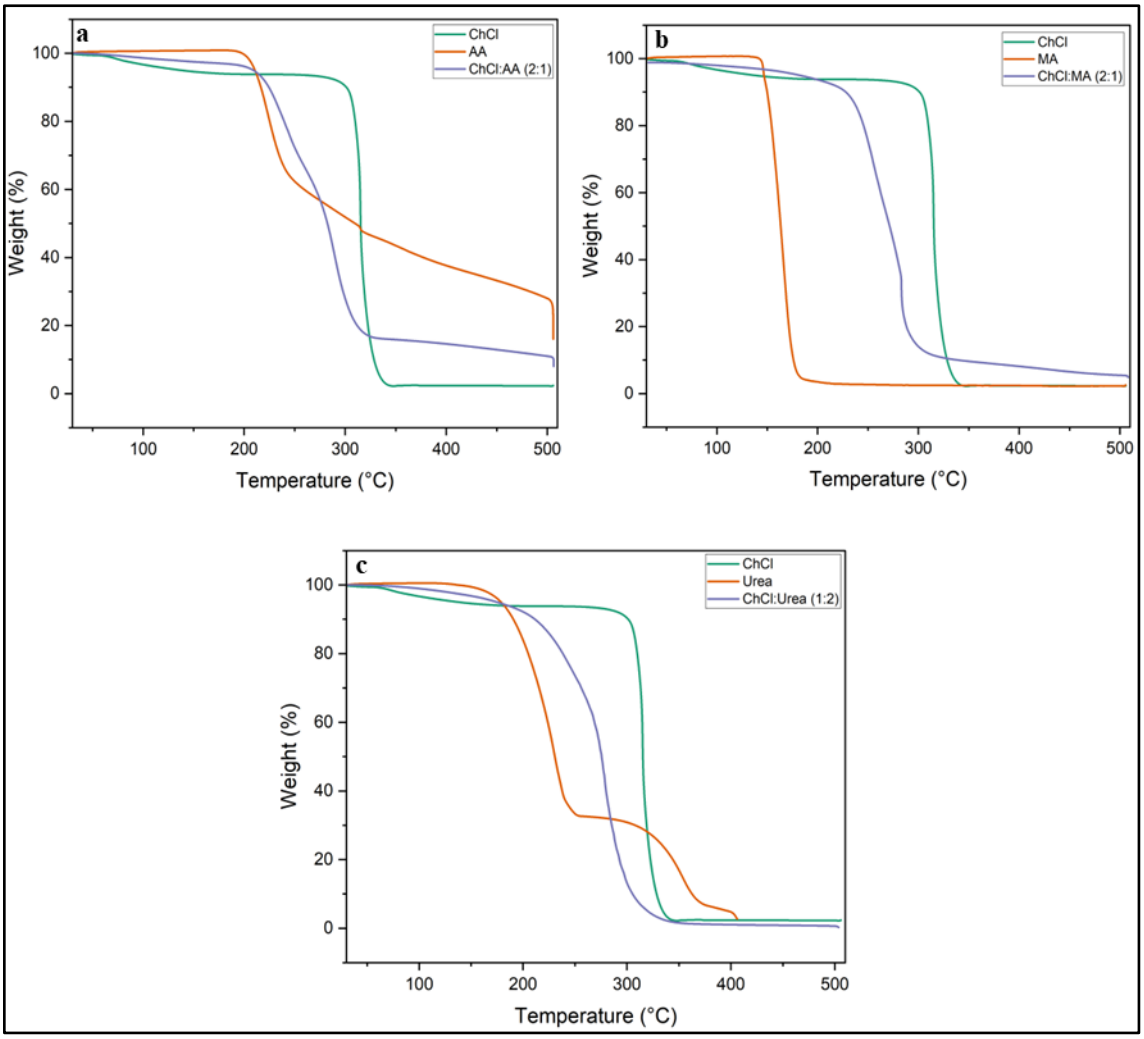

Figure 3. TGA curves of ChCl, AA and ChCl:AA (2:1) (a), ChCl, MA and ChCl:MA (2:1) (b), and ChCl, Urea and ChCl:Urea (1:2) (c)

The onset decomposition temperature (T_{onset}) is the point at which the highest decomposition rate occurs and the weight dependence on temperature curves tangent intersect. This maximum temperature at which DESs can remain in a liquid state without undergoing decomposition determines their applicability as solvents. As indicated in Table 2, the T_{onset} values for the DESs fall between those of their individual components, suggesting that the formation of DESs can enhance the thermal stability of HBDs since T_{onset} of the DESs are higher than T_{onset} of the HBDs. If more than one peak observed in TGA curves, only the temperature corresponding to the first peak is selected.

The T_{onset} values of the corresponding DESs are positively correlated with the stability of the HBDs. In other words, as the HBDs become more stable, the T_{onset} values of the DESs increase. From the results, AA has higher T_{onset} compared to urea, therefore, AA is more stable than urea. However, the thermal stability of DESs is also influenced by the molar ratio HBAs and HBDs. (Chen et al., 2018). T_{onset} of ChCl:urea is higher than ChCl:AA because the ratio of urea in the DES is 2 compared to AA in the DES which is 1. Therefore, ChCl:urea has the highest thermal stability compared to other two DESs. The positive ΔT_{onset} values observed between DESs and HBDs indicate an improvement in the thermal stability of HBDs. Maleic acid stands out with the highest ΔT_{onset} values which is 87.50 °C, indicating its exceptional ability to form a strong hydrogen bond network with ChCl (Chen et al., 2018).

Table 2. Decomposition temperature of DESs and HBDs

DESs	ChCl:HBD	T_{onset}/ °C			ΔT_{onset} DES-HBD/ °C
		DES	ChCl	HBD	
ChCl:AA	2:1	215.95	311.67	203.85	12.10
ChCl:MA	2:1	236.42	311.67	148.92	87.50
ChCl:Urea	1:2	257.74	311.67	198.75	58.99

* Condition: Heating rates: 20 °C/min

Differential scanning calorimetry (DSC) analysis

The DSC curves for all DES studied are shown in Figure 4. From Figure 4a, the glass transition temperature (Tg), identified by the baseline shift in the DSC curve, occurs at approximately 189 °C. In a DSC curve, the glass transition is recognized as a step change or a change in the slope of the baseline. It appears as a broad, gradual change in heat flow over a temperature range rather than a sharp peak or endothermic/exothermic event.

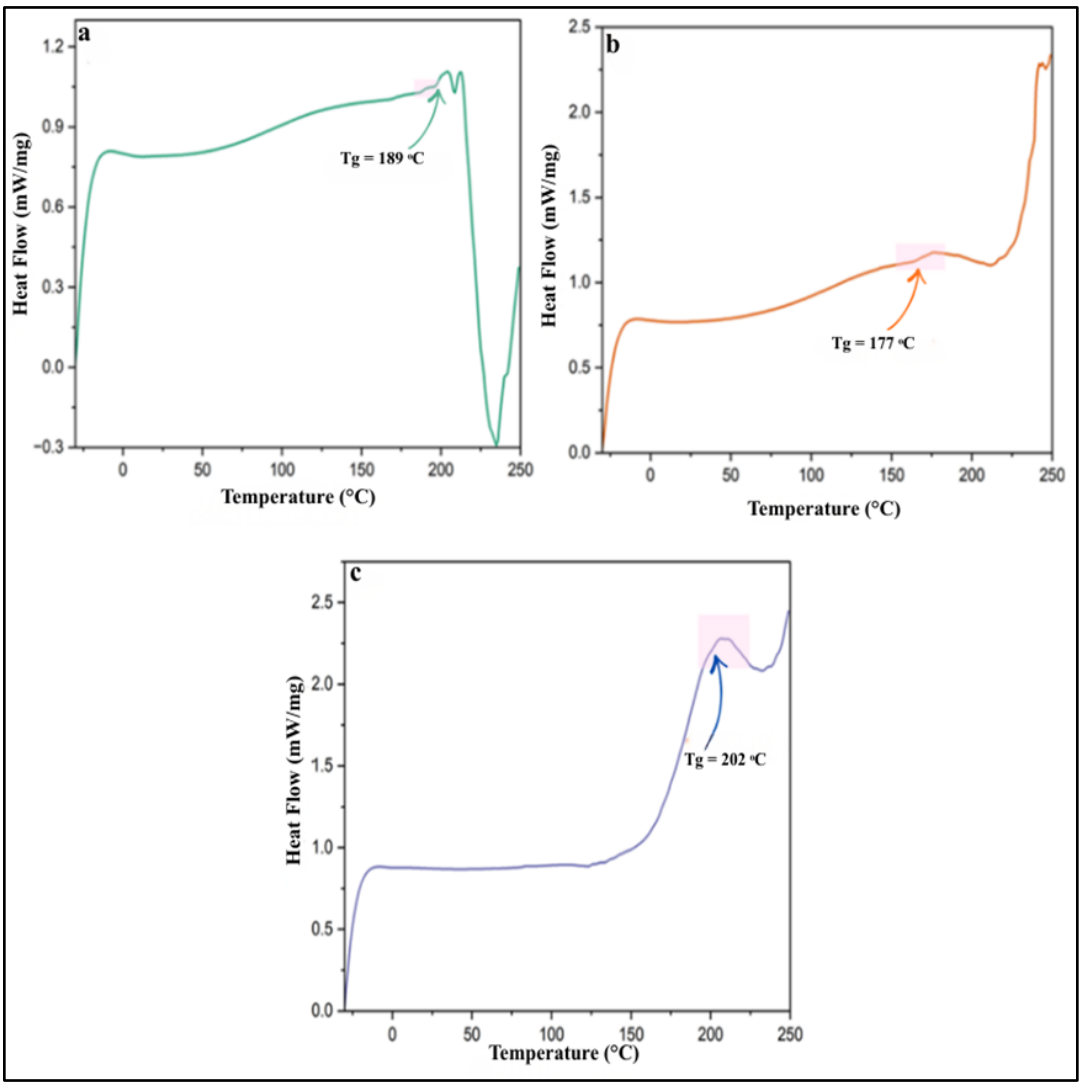

Figure 4. DSC curves for ChCl:AA (2:1) (a), ChCl:MA (2:1) (b), and ChCl:Urea (1:2) (c)

The glass transition is typically observed as an endothermic signal, meaning it absorbs heat from the surroundings. The glass transition in DES indicates the transition from a glassy state to a rubbery state as the temperature increases. It represents a change in the molecular arrangement and mobility within the DES. During the glass transition, the DES undergoes a shift from a rigid and relatively immobile state to a more flexible and mobile state. This was true since the ChCl:AA (2:1) was observed having

high viscosity at room temperature. As temperatures rise, the introduction of additional energy cause oxidative decomposition and degradation processes to take place (Leyva-Porras et al., 2019). As indicated by the figure 4a, ChCl:AA (2:1) start to degrade at 200 °C onwards. As shown in Figure 4b, ChCl:MA (2:1) exhibited a glass transition at 177 °C. Consistent with ChCl:AA (2:1), it displayed high viscosity at ambient temperature. ChCl:MA (2:1) also shows degradation when the temperature increased above 200°C. For ChCl:Urea (2:1), the crystallization of the amorphous glass began at - 40 °C and completed at –24 °C (Morrison et al., 2009). As shown in Figure 4c, an endothermic peak appeared in the DSC curve of ChCl:Urea (2:1) starting at 168 °C, and complete melting of the crystalline phase occurred at 207 °C, indicating its melting point. Similar to the other two DESs, ChCl:Urea (2:1) also exhibited degradation at temperatures above 207 °C. The DSC results are consistent with the TGA data, as all DESs begin to lose weight when the temperature exceeds 200 °C. For ChCl:Urea (2:1), the crystallization of the amorphous glass began at -40 °C and completed at -24 °C (Morrison et al., 2009). As shown in Figure 4c, an endothermic peak appeared in the DSC curve of ChCl:Urea (2:1) starting at 168 °C, and complete melting of the crystalline phase occurred at 207 °C, indicating its melting point. Similar to the other two DESs, ChCl:Urea (2:1) also exhibited degradation at temperatures above 207 °C. The DSC results are consistent with the TGA data, as all DESs begin to lose weight when the temperature exceeds 200 °C.

Visual Appearance of Synthesized DESs

Figure 1 shows the synthesized DESs at different molar ratios. The visual appearance of the DES mixtures varied depending on the hydrogen bond donor (HBD) and molar ratio used. ChCl:AA at a 2:1 molar ratio produced a homogeneous amber-colored liquid (Figure 1a), indicating successful formation of the eutectic mixture. ChCl:Urea at a 1:2 molar ratio also yielded a clear, homogeneous liquid (Figure 1c), which is consistent with this well-established DES formulation reported in the literature (Hansen et al. 2020). For ChCl:MA, the formation of a homogeneous DES was highly dependent on the molar ratio. Only the 2:1 ratio produced a homogeneous, clear liquid (Figure 1b), while the 1:1 and 1:2 ratios resulted in cloudy, heterogeneous mixtures (Figures 1d and 1e, respectively). The cloudy appearance suggests incomplete dissolution or phase separation, indicating that these ratios did not form stable eutectic systems under the synthesis conditions used. This observation suggests that the optimal molar ratio is critical for DES formation with maleic acid as the HBD, with the 2:1 ChCl:MA ratio being the most suitable composition for producing a stable, homogeneous DES.

Atomic Absorption Spectroscopy (AAS) analysis

Few parameters were selected to study the dissolution of ZnO in the DESs which are HBD, mass of ZnO, heating time, and heating temperature by using AAS. The results were presented in the percentage of dissolution.

Effect of HBD on dissolution of zinc oxide

Table 3 showed that ChCl:AA (2:1) have a higher solubility of ZnO than ChCl:MA (2:1) and ChCl:urea (1:2). This is explained by the fact that protons are present and serving as oxygen acceptors, which enhances dissolution. It was proposed that the higher acidity of DESs results in greater solubilities of MO compounds. This is due to the protons in the DESs acting as oxygen acceptors, leading to the breaking of metal-oxide bonds (Pateli et al., 2020). The solubility of MO showed a strong correlation with the activity of protons, with lower pH solutions frequently leading to increased solubility of MO compounds. However, the pH observed for ChCl:AA (2:1), ChCl:MA (2:1) and ChCl:urea (1:2) were 1.84, 0.65 and 10.1 respectively. Due to their distinct chemical characteristics and solubilities, ChCl:AA (2:1) can dissolve ZnO more effectively than ChCl:MA (2:1). AA has antioxidant properties and serves as a capable reducing agent (Li et al., 2020). It can react with ZnO, forming soluble zinc ascorbate complexes, which enhances its dissolution (Unaleroglu et al., 2002). Therefore, in this specific case, the ability of AA to dissolve ZnO better than MA is not solely attributed to the pH difference between the two acids but rather to their different chemical properties and their ability to interact with ZnO.

Table 3. Concentration of Zn in three different DESs

DES	Percentage of dissolution (%)
ChCl:AA (2:1)	80.6
ChCl:MA (2:1)	71.4
ChCl:Urea (1:2)	77.4

* Condition: Heating temperature: 50 °C, heating time: 48 hours, mass of ZnO: 5 mg

Effect of mass of zinc oxide to the dissolution

This parameter demonstrates how much ZnO can be dissolved by the DESs. From Table 4, it can be concluded that 2 mL of ChCl:AA (2:1) and ChCl:MA (2:1) can dissolve up to 20 mg of ZnO since their percentage of dissolution are 99 and 99.8% respectively. On the other hand, 2 mL of ChCl:urea (1:2) can only dissolve about 6 mg of ZnO. This result is agreed with the study from Richter & Ruck (2020) that found the acidic DES perform better than other DESs.

Table 4. Concentration of Zn in three different DESs at different mass of ZnO

DES	Percentage of dissolution (%)			
	5 mg	10 mg	15 mg	20 mg
ChCl:AA (2:1)	80.6	74.7	62.7	99.0
ChCl:MA (2:1)	71.4	75.5	68.9	99.8
ChCl:Urea (1:2)	77.4	66.8	45.3	30.2

*Condition: Heating temperature: 50 °C, heating time: 48 hours

Effect of heating time on dissolution of zinc oxide

Table 5 shows the concentration of Zn in ChCl:AA (2:1) and ChCl:urea (1:2) increased when the heating time increase. Since dissolution typically occurs at the surface of the solid material, increasing the dissolution time allows for more surface area of ZnO to be exposed to the solvent, facilitating further dissolution (Siew, 2016). For ChCl:MA (2:1), the percentage of dissolution at 18 hours is almost the same as at 20 hours. However, after 20 hours, the percentage of dissolution is decreased. It was expected that the DES may reach a state of saturation, where the concentration of dissolved Zn becomes relatively stable. At this point, further heating may not significantly increase the dissolution. Other than that, since the dissolution of MO in DES is typically a kinetic process, the dissolution rate influenced by the contact between the MO and the DES and the diffusion of metal ions through the DES. Initially, when the heating is started, the dissolution rate may be high as the system reaches an equilibrium state. However, as time progresses, the dissolution rate may slow down due to the decreasing surface area of the MO, limited diffusion of metal ions, or changes in the dissolution mechanism. Therefore, 18 hours was chosen as an optimum heating time for ChCl:MA (2:1). According to previous study from Jangir et al. (2021) and Abbott et al. (2006), heating time that are required for the dissolution of ZnO are 24 hours and 48 hours, respectively.

Table 5. Concentration of Zn in three different DESs at various heating time

DES	Percentage of dissolution (%)			
	18 hours	20 hours	24 hours	48 hours
ChCl:AA (2:1)	60.8	65.4	79.0	80.6
ChCl:MA (2:1)	77.2	77.8	66.8	71.4
ChCl:Urea (1:2)	28.8	43.4	59.6	77.4

*Condition: Heating temperature: 50 °C, mass of ZnO: 5 mg

Effect of heating temperature on dissolution of zinc oxide

Table 6 shows that when ChCl:AA (2:1) was heated at 70 °C, it dissolves more readily, and raising the temperature no longer causes the solubility to increase. While for ChCl:urea (1:2), as the heating temperature was at 80 °C, the amount of dissolved Zn noticeably rises, demonstrating the enhanced solubility of ZnO in ChCl:urea (1:2) at higher temperatures due to the additional energy which is assist for breaking the lattice structure of the ZnO. Furthermore, higher temperatures can improve the mobility and diffusion of species within the DES, including metal ions. When the mobility increases, metal ions

are easier to be transported away from the MO surface, thus enhance the dissolution.

For ChCl:MA (2:1), the higher solubility of Zn was recorded when the heating temperature was 60 °C. Upon elevating the heating temperature to 80 °C, there is a slight decline observed in the concentration of Zn. This may be because at higher temperatures, the DES components may undergo chemical reactions such formation of complex naming zinc maleate that affect the dissolution process (Yudanova et al., 2018). This complexation can decrease the solubility of ZnO by reducing the availability of dissolved zinc species in the solvent. As the complex forms, a portion of the zinc ions in the solution becomes incorporated into the complex, reducing the concentration of freely dissolved zinc ions.

Table 6. Concentration of Zn in three different DESs at various heating temperature

DES	Percentage of dissolution (%)			
	50 °C	60 °C	70 °C	80 °C
ChCl:AA (2:1)	80.6	79.2	84.8	84.8
ChCl:MA (2:1)	71.4	84.6	78.0	81.8
ChCl:Urea (1:2)	77.4	72.0	73.8	89.0

*Condition: Heating time: 48 hours (ChCl:AA and ChCl:Urea), 18 hours (ChCl:MA), mass of ZnO: 5 mg

Conclusion

The DESs ChCl:AA (2:1), ChCl:MA (2:1), and ChCl:Urea (1:2) were successfully synthesized and characterized, with FTIR confirming their eutectic nature through the presence of peaks from both HBA and HBD, slightly shifted due to intermolecular interactions. Thermal analyses (TGA and DSC) demonstrated that all DESs remained stable up to 200 °C. Dissolution studies showed that ZnO exhibited the highest solubility in ChCl:AA (2:1), followed by ChCl:MA (2:1), while ChCl:Urea (1:2) dissolved significantly less under the same conditions. Optimal dissolution conditions varied: 70 °C for 48 h for ChCl:AA (2:1), 60 °C for 18 h for ChCl:MA (2:1), and 80 °C for 48 h for ChCl:Urea (1:2). These findings suggest that complex formation during dissolution may influence solubility, highlighting the need for further mechanistic and kinetic studies to optimize ZnO dissolution and enhance the sustainability of these DES systems.

Acknowledgement/Funding

Authors would like to acknowledge the financial support given by School of Chemical Sciences, Universiti Sains Malaysia.

Author Contribution

Samer Sami Aburub: Writing – review & editing; formal analysis; visualization. Nur Aida Mohd Zakhir: Methodology; Writing – original draft. Nurul Yani Rahim: Conceptualization; Investigation; Supervision; Validation; Writing – review & editing

Conflict of Interest

Authors declare no conflict of interest

Declaration on the Use of Generative AI

Authors declare no generative AI used in the manuscript.

References

Abbott, A. P., Capper, G., Davies, D. L., McKenzie, K. J., & Obi, S. U. (2006). Solubility of metal oxides in deep eutectic solvents based on choline chloride. *Journal of Chemical and Engineering Data*, *51*(4), 1280–1282. https://doi.org/10.1021/je060038c

Al-Risheq, D. I. M., Nasser, M. S., Qiblawey, H., Ba-Abbad, M. M., Benamor, A., & Hussein, I. A. (2021). Destabilization of stable bentonite colloidal suspension using choline chloride based deep eutectic solvent: Optimization study. *Journal of Water Process Engineering*, *40*, 101885. https://doi.org/10.1016/j.jwpe.2020.101885

Amphlett, J. T. M., & Choi, S. (2019). Metal Oxide Solubility in Deep Eutectic Solvents Applications in Decontamination in Decommissioning. *Korean Radioactive Waste Society Spring Conference*, 287–288.

Chen, W., Xue, Z., Wang, J., Jiang, J., Zhao, X., & Mu, T. (2018). Investigation on the thermal stability of deep eutectic solvents. *Acta Physico-Chimica Sinica*, *34*(8), 904–911. https://doi.org/10.3866/PKU.WHXB201712281

Chik, M. A. W., Shafie, M. H., Hanaphi, R. M., & Yusof, R. (2025). Unlocking Choline Dihydrogen Citrate as a New Potential Hydrogen Bond Acceptor Replacing Choline Chloride in Malonic Acid-Based Deep Eutectic Solvent Formulation. *Malaysian Journal of Chemistry, 27(3), 149-172. https://doi.org/10.55373/mjchem.v27i3.149*

Delgado-Mellado, N., Larriba, M., Navarro, P., Rigual, V., Ayuso, M., García, J., & Rodríguez, F. (2018). Thermal stability of choline chloride deep eutectic solvents by TGA/FTIR-ATR analysis. *Journal of Molecular Liquids*, *260*, 37–43. https://doi.org/10.1016/j.molliq.2018.03.076

Hansen, B. B., Spittle, S., Chen, B., Poe, D., Zhang, Y., Klein, J. M., Horton, A., Adhikari, L., Zelovich, T., Doherty, W. B., Gurkan, B., Maginn, J. E., Ragauskas, A., Dadmun, M., Zawodizinski, A. T., Baker, A. G., Tuckerman, E. M., & Sangoro, J. R. (2020). Deep eutectic solvents: a review of fundamentals and applications. *Chemical reviews, 121(3)*, 1232-1285. https://doi.org/10.1021/acs.chemrev.0c00385

Jangir, A. K., Sethy, P., Verma, G., Bahadur, P., & Kuperkar, K. (2021). An inclusive thermophysical and rheology portrayal of deep eutectic solvents (DES) for metal oxides dissolution enhancement. *Journal of Molecular Liquids*, *332*, 115909. https://doi.org/10.1016/j.molliq.2021.115909

Joseph, J., & Jemmis, E. D. (2007). Red-, blue-, or no-shift in hydrogen bonds: A unified explanation. *Journal of the American Chemical Society*, *129*(15), 4620–4632. https://doi.org/10.1021/ja067545z

Jurić, T., Uka, D., Holló, B. B., Jović, B., Kordić, B., & Popović, B. M. (2021). Comprehensive physicochemical evaluation of choline chloride-based natural deep eutectic solvents. *Journal of Molecular Liquids*, *343*, 116968. https://doi.org/10.1016/j.molliq.2021.116968

Leyva-Porras, C., Cruz-Alcantar, P., Espinosa-Solís, V., Martínez-Guerra, E., Piñón-Balderrama, C. I., Martínez, I. C., & Saavedra-Leos, M. Z. (2019). Application of differential scanning calorimetry (DSC) and modulated differential scanning calorimetry (MDSC) in food and drug industries. *Polymers*, *12*(1), 5. https://doi.org/10.3390/polym12010005

Li, Q., Li, Y., Li, H., Yan, X., Han, G., Chen, F., Song, Z., Zhang, J., Fan, W., Yi, C., Xu, Z., Tan, B., & Yan, W. (2020). Highly luminescent copper nanoclusters stabilized by ascorbic acid for the quantitative detection of 4-aminoazobenzene. *Nanomaterials*, *10*(8), 1–15. https://doi.org/10.3390/nano10081531

Li, X., & Binnemans, K. (2021). Oxidative dissolution of metals in organic solvents. *Chemical Reviews, 121(8),* 4506-4530. https://doi.org/10.1021/acs.chemrev.0c00917

Li, Y., Li, Y., Li, H., Fan, X., Yan, H., Cai, M., Xu, X., & Zhu, M. (2022). Insights into the tribological behavior of choline chloride—urea and choline chloride—thiourea deep eutectic solvents. *Friction*, *11*, 76–92. https://doi.org/10.1007/s40544-021-0575-4

Ling, J. K. U., Chan, Y. S., Nandong, J., Chin, S. F., & Ho, B. K. (2020). Formulation of choline chloride/ascorbic acid natural deep eutectic solvent: Characterization, solubilization capacity and antioxidant property. *LWT*, *133*, 110096. https://doi.org/10.1016/j.lwt.2020.110096

Ling, J. K. U., & Hadinoto, K. (2022). Deep Eutectic Solvent as Green Solvent in Extraction of Biological Macromolecules: A Review. *International Journal of Molecular Sciences*, *23*(6), 3381. https://doi.org/10.3390/ijms23063381

Markiewicz, R., & Jurga, S. (2011). Ionic liquids and deep eutectic solvents in the preparation of nanostructures. *Physical Chemistry Chemical Physics*, *44*(11), 7108–7146.

Morrison, H. G., Sun, C. C., & Neervannan, S. (2009). Characterization of thermal behavior of deep eutectic solvents and their potential as drug solubilization vehicles. *International Journal of Pharmaceutics*, *378*(1–2), 136–139. https://doi.org/10.1016/j.ijpharm.2009.05.039

Noman, M. T., Amor, N., & Petru, M. (2022). Synthesis and applications of ZnO nanostructures (ZONSs): a review. *Critical Reviews in Solid State and Materials Sciences*, *47*(2), 99–141. https://doi.org/10.1080/10408436.2021.1886041

Pateli, I. M., Thompson, D., Alabdullah, S. S. M., Abbott, A. P., Jenkin, G. R. T., & Hartley, J. M. (2020). The effect of pH and hydrogen bond donor on the dissolution of metal oxides in deep eutectic solvents. *Green Chemistry*, *22*(16), 5476–5486. https://doi.org/10.1039/d0gc02023k

Richter, J., & Ruck, M. (2020). Synthesis and dissolution of metal oxides in ionic liquids and deep eutectic solvents. *Molecules*, *25*(1), 78. https://doi.org/10.3390/molecules25010078

Sakhno, T. V., Barashkov, N. N., Irgibaeva, I. S., Mendigaliyeva, S., & Bostan, D. S. (2020). Ionic Liquids and Deep Eutectic Solvents and Their Use for Dissolving Animal Hair. *Advances in Chemical Engineering and Science*, *10*(01), 40–51. https://doi.org/10.4236/aces.2020.101003

Siew, A. (2016). Dissolution Testing. *Pharmaceutical Technology*, *40*(11), 56–64.

Taghizadeh, S. M., Berenjian, A., Zare, M., & Ebrahiminezhad, A. (2020). New perspectives on iron-based nanostructures. *Processes*, *8*(9), 1128. https://doi.org/10.3390/PR8091128

Unaleroglu, C., Zumreoglu-Karan, B., & Mert, Y. (2002). Zinc ascorbate: a combined experimental and computational study for structure elucidation. *Journal of Molecular Structure*, *605*, 227–233. www.elsevier.com/locate/molstruc

Wang, H., Liu, S., Zhao, Y., Wang, J., & Yu, Z. (2019). Insights into the Hydrogen Bond Interactions in Deep Eutectic Solvents Composed of Choline Chloride and Polyols. *ACS Sustainable Chemistry and Engineering*, *7*(8), 7760–7767. https://doi.org/10.1021/acssuschemeng.8b06676

Yudanova, L. I., Logvinenko, V. A., Korol'kov, I. V., Ishchenko, A. V., & Rudina, N. A. (2018). Thermal Decomposition in Systems of Acid Zn(II), Co(II), and Ni(II) Maleates with the Formation of Metallic Nanoparticles. *Russian Journal of Physical Chemistry A*, *92*(11), 2247–2252. https://doi.org/10.1134/S003602441811047X